

Harvard-Smithsonian Center for Astrophysics  
Precision Astronomy Group

To: Distribution 14 February 1997 TM97-01  
From: R.D. Reasenberg  
Subject: Bias in the Estimate of Star Coordinates due to Spatial Variation in Detector  
Sensitivity -- Static Case

## I. Introduction.

As discussed in TM96-04, we consider a diffraction-limited astrometric instrument with a rectangular aperture of length  $S$  and height  $H$ , in which a central region of length  $\gamma S$  would not be used. See Fig. 1. The analysis is conducted in the context of FAME, a spaceborne survey instrument, but most results are independent of that context. We assume that a diffraction-limited image falls on an array detector (e.g., a CCD); thus the optical instrument is either a telescope or a Fizeau interferometer, but not a Michelson interferometer. We further assume that the detector has a nonuniform detection sensitivity, and that this non-uniformity may depend on (optical) wavelength. The analysis is done in the bright-star limit and ignores important contributions to the loss of fringe visibility, including pixelation and optical aberration.

In Section II, we consider the bias in the estimate of a star coordinate due to a periodic variation in the detector sensitivity. The analytic form of the result, which is based on the observation of the full diffraction pattern, is shown to be accessible by a heuristic approach in Section III. Results from measurements of real CCDs are introduced in Section IV. These measurement results set the scale of the problem, as discussed at the end of Section II. In Section V, we consider the effect of observing a limited portion of the diffraction pattern. Finally, in Section VI, I attempt to put some of the results in perspective and add a few concluding notes. I find that Time-Delayed Integration (TDI) is required to suppress the bias by only a small factor, which it surely will do. In particular, the factor of  $\cos(\varphi)$  in Eq. (13) averages to zero as the center of the diffraction pattern sweeps over a single pixel. Even if there are effects that cause this suppression to be imperfect, the bias due to CCD sensitivity variation will not matter for FAME.

## II. Estimation Analysis.

In TM96-04, we considered the information rate of the estimator used to determine coordinates of the star. Here we consider the bias,  $\Delta$ , in the estimate of a star coordinate that would result from a spatial variation in the sensitivity of the detector array. We treat this bias as a perturbation of the estimated star coordinate  $\psi$  (the “location” of the star in the  $p$  direction) and calculate it using the weighted-least-squares (WLS) estimator.

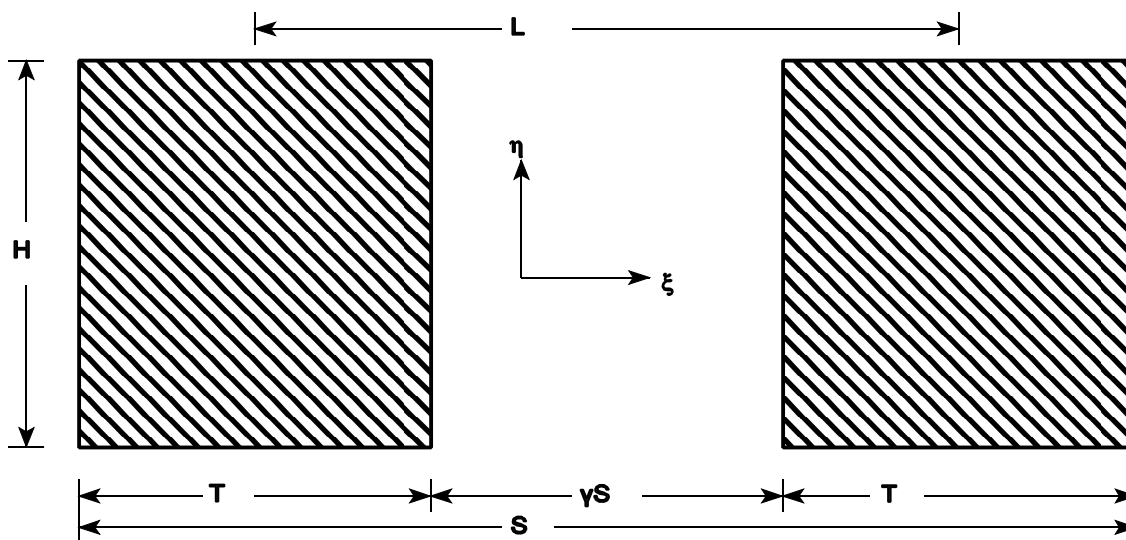


**Figure 1.**  $W$ , the aperture or windowing function, is shown shaded. (From TM96-04)

$$\Delta = B^{-1} V \quad (1)$$

In Eq. (1),  $B$  is the “WLS coefficient matrix” given in Eq. (11) of TM96-04 and

$$V = A^\dagger R^{-1} r = \int_{-\infty}^{\infty} \int_{-\infty}^{\infty} dpdq \left[ \frac{\partial M}{\partial \psi} \right] \frac{1}{M} r \quad (2)$$

where  $A$  is the sensitivity matrix (i.e., partial of the observable,  $M$ , with respect to the parameter,  $\psi$ ),  $R$  is the (data) noise covariance matrix (in this case, due to photon counting statistics),  $r$  is the perturbation residual (due to the nonuniformity of the detector sensitivity), the observable,  $M$ , is the photon count density, and  $p$  and  $q$  are the image-space angles with respect to the incoming direction (taken to be approximately perpendicular to the aperture plane. Angles  $p$  and  $q$  map into position on the focal plane *via* effective focal lengths, which are expected to be different for the two coordinates). Note that this is a single parameter (scalar) case and that I have used an approximation,  $R = \sigma^2(M) = M$ , which neglects read noise. This is reasonable since we are principally concerned with bias for stars that are measured with high precision; these are bright and, for them, read noise is negligible.

We represent the non-uniformity of the detector sensitivity by a factor that is periodic in position:  $1 + \alpha \sin(kp + \varphi)$ . Then

$$r = M \alpha \sin(kp + \varphi) \quad (3)$$

where  $k$  is the wave vector for the perturbation, which has fractional amplitude  $\alpha$ . In practice,  $r$  would be a superposition of perturbations, and might need to be represented as a power spectral density. In order to evaluate Eq. (2), we apply Eqs. (2), (4), (7), and (10) of TM96-04

$$M(p,q) = \frac{\tau U^2}{h\nu} \quad (4)$$

$$U(p,q) = \frac{\sqrt{F}}{\lambda} J_c J_s \quad (5)$$

$$J_q = \int_{-\infty}^{\infty} J_c^2 dq = \int_{-\infty}^{\infty} \left[ \frac{\sin(\pi q H / \lambda)}{\pi q / \lambda} \right]^2 dq = H\lambda \quad (6)$$

$$J_s = \int_{-S/2}^{S/2} e^{-ikp\xi} d\xi - \int_{-\gamma S/2}^{\gamma S/2} e^{-ikp\xi} d\xi = \frac{\sin(\pi p S / \lambda) - \sin(\pi p \gamma S / \lambda)}{\pi p / \lambda} \quad (7)$$

In the above equations,  $J_s$  is the quantity known as  $J_i$  in TM96-04,  $F$  is the optical flux (power per unit area),  $\lambda$  is the optical wavelength,  $\xi$  and  $\eta$  are coordinates in the aperture plane, and  $U(p,q)$  is the field, with the (complex) time-dependent part removed, and has units of root power density.<sup>1</sup> Note that the analysis is carried out for a single optical wavelength. When considering the full optical band pass,  $\alpha$  would become  $\alpha(\lambda)$  in addition to having a dependance on  $k$ .

By making the required substitutions, we obtain

---

1)  $U$  has units of root (power per solid angle), where solid angle is measured in  $p$  and  $q$ .

$$V = \frac{2\tau\alpha HF}{h\nu\lambda} I_v$$

$$I_v = \int_{-\infty}^{\infty} dp J_s \frac{\partial J_s}{\partial p} \sin(kp + \varphi) \quad (8)$$

To evaluate Eq. (8), we differentiate Eq. (7)

$$\frac{\partial J_s}{\partial p} = \frac{S}{p} \left[ \cos\left(\frac{\pi p S}{\lambda}\right) - \gamma \cos\left(\frac{\pi p \gamma S}{\lambda}\right) \right] - \frac{\lambda}{\pi p^2} \left[ \sin\left(\frac{\pi p S}{\lambda}\right) - \sin\left(\frac{\pi p \gamma S}{\lambda}\right) \right] \quad (9)$$

and expand  $\sin(kp + \varphi) = \sin(kp)\cos(\varphi) + \cos(kp)\sin(\varphi)$ . By symmetry, the  $\sin(\varphi)$  term is zero. Then, with the help of Mathcad,<sup>®1</sup> we find

$$I_v = \cos(\varphi) \frac{\pi S^2}{8} G(\gamma, f) \quad (10)$$

where  $f \equiv \lambda k / \pi S$  and  $G(\gamma, f)$  is given in Appendix A. (Note that  $f$  is the number of cycles of perturbation in  $2\lambda/S$ , the angular width (between first nulls) of the central fringe of an unobscured fringe pattern,  $\gamma=0$ .) Here I provide only a special case

$$G(0, f) = f [2|f| - |f-2| - |f+2|] \quad (11)$$

which has peak values of -2 and 2 at  $f = 1$  and  $f = -1$  respectively, and is zero at  $f = 0$  and  $|f| > 2$ . Figures 2 and 3 show  $G$  for six values of  $\gamma$ , the last of which is  $G(0, f)$ .

An expression for  $B$  is given in Eq. (14) of TM96-04

$$B = \frac{4\pi^2 \tau FHS^3}{3h\nu \lambda^2} (1-\gamma^3) \quad (12)$$

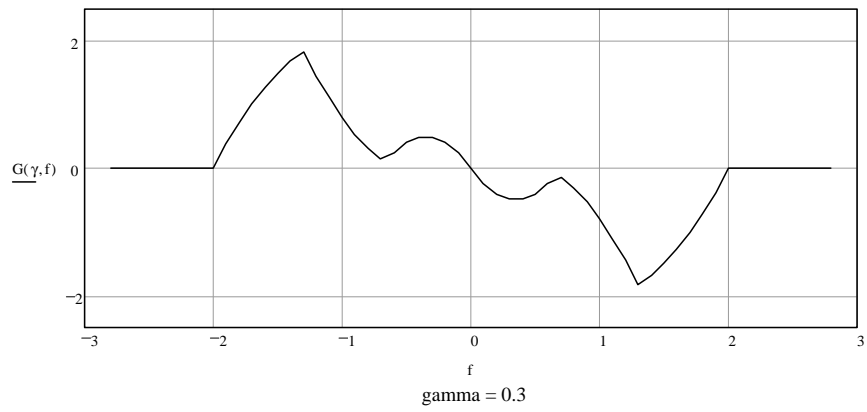
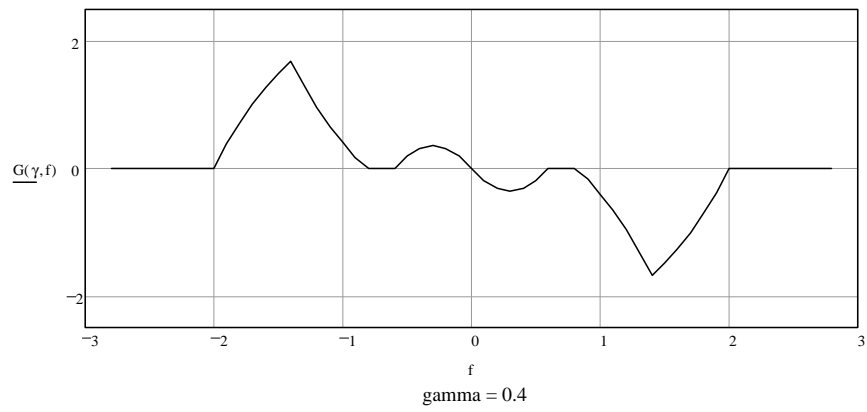
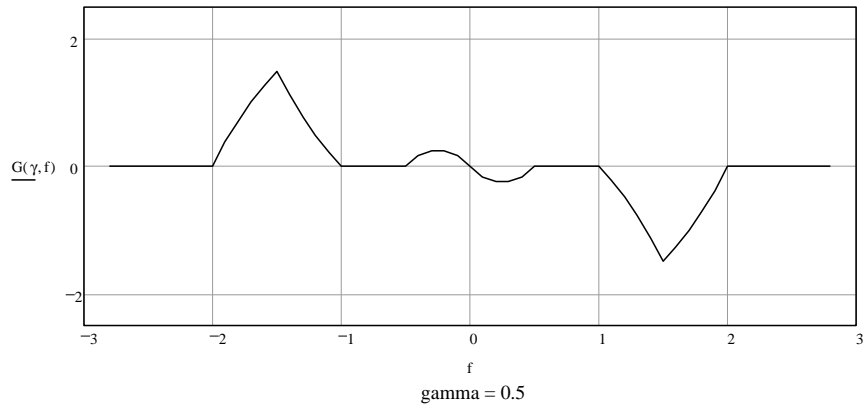


Figure 2. The function  $G(\gamma, f)$  for  $\gamma = 0.5$ ,  $0.4$ , and  $0.3$ .

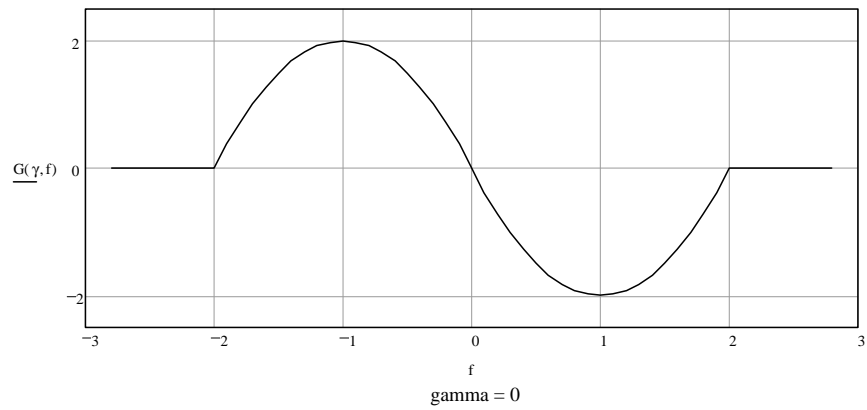
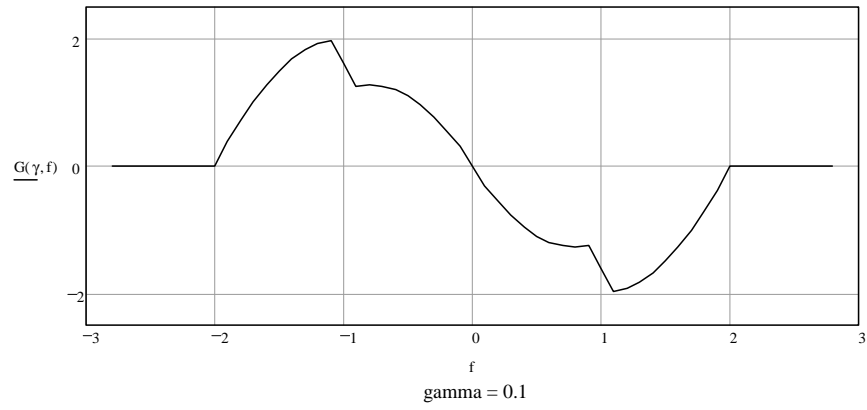
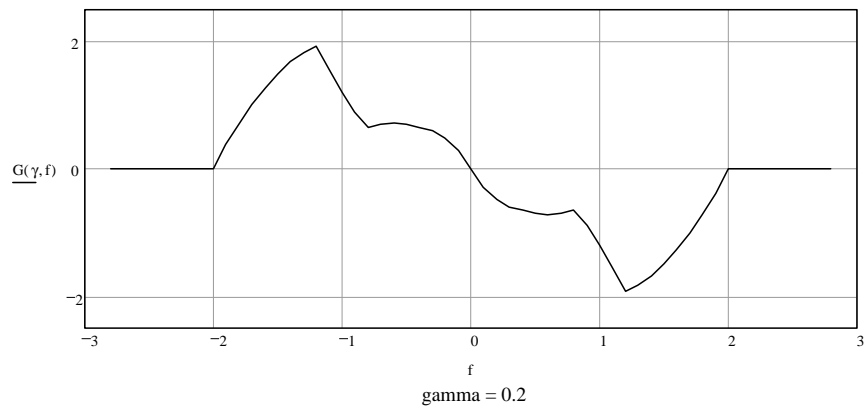


Figure 3. The function  $G(\gamma, f)$  for  $\gamma = 0.2$ ,  $0.1$ , and  $0$ .

By combining this with Eqs. (1), (8), and (10), we obtain

$$\Delta = \Delta_0 \cos(\varphi)$$

$$\Delta_0 = \frac{3\alpha}{16\pi(1-\gamma^3)} \frac{\lambda}{S} G(\gamma, f) \quad (13)$$

From Eqs. (11) and (13) and from Figs. 2 and 3, it is clear that  $|f| = 2$  is a significant threshold. We relate this to the angular coordinate (which maps to the detector plane via a focal length) by

$$k p^* \Big|_{f=2} = 2\pi \quad (14)$$

which yields  $p^* = \lambda / S$ . (Cf Eq. (8).) Thus, periodic structures with periods shorter than  $p^* = \lambda / S$  do not contribute to  $\Delta$ , i.e., they do not perturb the estimate of the star coordinate. For a perturbative structure with wavelength equal to the pixel size, this cutoff corresponds to two pixels in the full width (at first zeros) of the central lobe of the diffraction pattern of an unobscured aperture ( $\gamma=0$ ). Since one would normally expect to have more like four pixels in the central lobe, the problem (of bias induced by pixel-scale variation of sensitivity) appears to be academic. However, as discussed in Section VI, this independence from CCD sensitivity variation is valid only if the full diffraction pattern (corresponding to the infinite limits in Eq. (8)) is included in the analysis. This is not expected to be a good approximation for the optimized instrument. If we were not planning to use TDI, it would be useful to investigate windowing functions that reduce the contribution to  $\Delta$ .

Equation (13) can be usefully normalized by  $\sigma_1$  (the standard deviation of the estimate of the star position in the scan direction based on a single observation), which we get from Eq. (14) *et seq* of TM96-04.

$$\frac{\Delta_0}{\sigma_1} = \frac{\alpha\sqrt{3N}}{8\sqrt{(1-\gamma^3)(1-\gamma)}} G(\gamma, f) \quad (15)$$

where  $N$  is the number of detected photons. Assuming a mag 10 star observed over an optical band pass of 0.4 to 0.9 microns for 1 sec at an overall detection efficiency of  $\eta = 0.16$  (including the effect of  $\gamma=0.4$ ), we find  $N = 6 \cdot 10^4$ . Then, for  $\alpha = 0.1$  and  $\gamma = 0.4$ , the ratio in the above equation is 7.1  $G$ . (Here we are neglecting the  $\lambda$ -dependance of  $\Delta$  in order to get a quick result that sets the scale of the problem.) Note that for  $\gamma = 0.4$ , the peak value of  $G$  is 1.7; with  $S = 60$  cm,  $\lambda = 0.5$  micron, and  $\alpha = 0.1$ , the corresponding bias is 19 mas, far more than would be acceptable for FAME. We return to this subject in Section VI.

### III. A Heuristic Derivation

The 21 term expression for  $G$  given in Appendix A is less than transparent. Further, it is unusual for an analytic result to have a finite domain with structure and be zero elsewhere. In this section, I show that the form of  $G$  can easily be found, without resort to messy equations.

Equation (8) has the form of a Fourier (inverse) transform. Similarly,  $J_s$  is the Fourier transform of the difference of two rectangular pulses. Let  $\mathcal{F}$  ( $\mathcal{F}^{-1}$ ) represent a Fourier (Fourier inverse) transform. Then Eq. (8) takes the form

$$I_v = \mathcal{F}^{-1} \left[ \mathcal{F}(\text{rec}(\xi 2/S) - \text{rec}(\xi 2/\gamma S)) \partial_{\xi} \mathcal{F}(\text{rec}(\xi 2/S) - \text{rec}(\xi 2/\gamma S)) \right] \quad (16)$$

where  $\text{rec}(x)$  is one for  $|x| < 1$  and zero for  $|x| > 1$ . We may apply the following theorems: 1) The transform of a product is the convolution of the transforms. 2) The derivative of the transform is the transform of the product of the independent variable and the original function. Then Eq. (16) simplifies to the convolution of the aperture and the product of the aperture and a linear ramp passing through the origin. To show that the function shapes in Figs. 2 and 3 are thus obtained is an exercise with graph paper, which is relatively simple for  $\gamma=0$ . The extension to apertures of other shapes shows that all finite apertures yield a finite cutoff to the spatial frequency of the detector perturbation that affects the estimate of the star position (providing that there is no read noise and no pixelation and that the observation window is unbounded).

#### IV. Real CCD detectors and Induced Bias.

For a photon striking a CCD, there are two position-dependent types of departure from ideal detection. First, the detected charge may be collected in a pixel different from the one in which the photon was converted to an electron-hole pair. Such an “effective blur” may be modeled by including it with the description of blur by the optics. There may be an enhanced effect near the pixel edges, due for instance to buried electrodes, but increasing the overall effective blur to model it is likely to be adequate. Second, the QE, defined as the probability of detection with charge collected in *any* pixel, may vary with position. The latter is the subject of the present memorandum.

Measurements of CCD spatial response have been made by a variety of means. Marchywka and Socker (1992) measure the modulation transfer function by illuminating the CCD with an interference pattern generated with laser light. They describe the results of a study of the Kodak KAF-1400 imager, which is front-side illuminated. They find very deep intra-pixel sensitivity modulation. Since we are not considering a detector that is front-side illuminated, we do not further consider this work.

Jorden et al. (1994) demagnify ten fold an illuminated hole, which they translate to scan a ( $\approx 3$  micron diameter) spot of light across a CCD detector. They studied both frontside-illuminated thick (EEV) and backside-illuminated thin (Tek) detectors. The backside-illuminated Tektronix 1024 uses a buried channel, three phase electrode structure. It has  $24 \times 24$  micron pixels and 15 microns of silicon substrate. The paper reports a study of the Tek1042 with both 500 and 800 nm radiation; scans were in both the column and row directions. Jorden et al.

present the total energy received by a nine-pixel block as the spot is scanned across the central pixel. Peak-to-valley variations range from 12% (along the column, 800 nm) to 4% (across the columns, 500 nm). They have done no further work and Jorden (1996) knows of no other measurements of this kind. He has kindly offered me a copy of the data at all wavelengths. (But since we will be using different detectors, I have not pursued these data.)

In the manufacture of a CCD, the pixel pattern may be generated from a segment of the needed pattern by step-and-repeat operations. An error in the step size or an irregularity in the repeated pattern would give rise to large-scale structure in the full array. Similarly, an error produced by variations in the photoresist coating thickness or in the exposure of the photoresist could map into a large-scale CCD error. As of the date of this memorandum, I have no specific information about such structures.

#### V. Effect of Detecting a Limited Portion of the Diffraction Pattern.

Equation (8) was written under the assumption that all of the diffracted light would be detected -- the infinite detector case. As a practical matter, the region of the detector from which data are taken is limited by the combined costs of computation and (spacecraft) telecommunications and by the diminishing returns from data taken far from the center of the diffraction pattern. Unfortunately, the equivalent of  $G(\gamma, f)$  does not go to zero for  $f > 2$  when the limits in Eq. (8) are made finite. To see this, we consider the changes to Eq. (16) that come from a limited data span in the scan direction. If the data span is to have a full width  $2u\lambda/S$ , then

$$Z(f, u) = \mathcal{F}^{-1} \left[ \text{rec}(pS/u\lambda) \left[ \mathcal{F}(\text{rec}(\xi 2/S) - \text{rec}(\xi 2/\gamma S)) \partial_{\xi} \mathcal{F}(\text{rec}(\xi 2/S) - \text{rec}(\xi 2/\gamma S)) \right] \right] \quad (17)$$

Applying the Fourier-transform theorems of Section III, we find that  $Z(f, u)$  is the convolution of  $I_v$  and the Fourier transform of  $\text{rec}(pS/u\lambda)$ , which is a sinc function and falls off inversely with  $f$ . Thus, unlike  $I_v$ ,  $Z(f, u)$  does not go to zero at finite  $f$ . (An attempt to obtain an analytic description of  $Z(f, u)$  caused Mathcad to give up. However, Murison (1997) was able to perform the required analysis using Maple.<sup>®1)</sup> In Appendix B, I present an investigation of a simplified model in which  $G$  is replaced by  $G^*$ , which comprises a pair of contiguous, equal-size rectangular pulses of opposite sign. The simple sharp-edged form of  $G^*$  probably results in an overestimate of  $Z$ . This model, which uses an asymptotic expression for the Sine Integral, shows that  $Z(f, u)$  falls off as  $2/\pi^2 u f$ , for large  $f$ . For  $f=4$  and  $u=2$ , the suppression factor found in Appendix B is 40.

## VI. Concluding Remarks.

In setting the “plate scale” for FAME, the first question is: How big should the image be compared to the pixel size? If the image is too small, there is a loss of fringe visibility and thus of information. If the image is too large, an array of fixed size sees too little of the sky, and again there is a loss of information. The required optimization will be addressed in a forthcoming memo by J.D. Phillips. Here, we have seen that there is another consideration -- systematic error -- that may set image size.

We have considered a static diffraction-limited star image on a discretized detector (e.g., a CCD) and found that a periodic error in the sensitivity of the detector may result in a biased estimate of the star position. For the case of an unbounded observing window, Figs. 2 and 3 show that, independent of the value of  $\gamma$ , the bias in star position goes to zero when there are two or more cycles of the periodic variation in sensitivity across the portion of the detector spanned by the central peak of the unobstructed aperture. To prevent a bias in the wide-band case, the criterion would need to be met for the shortest optical wavelength that could significantly affect the position measurement. Detector cutoff ( $\approx 250$  nm for Si) could be used. However, a longer wavelength cutoff, and correspondingly larger pixels, may be preferred. In this case, transverse dispersion or a band-limiting filter may be desirable.

To conserve resources in the FAME mission, we expect to save and process as small a number of pixels as possible, i.e., have a small observing window. In this case, even if the periodic error is of high frequency, we find that the bias is non-zero and falls off as  $1/f$ , the total number of cycles of the sensitivity variation contained in the observing window. For a low-frequency periodic error, the limited observing window has negligible effect on the bias.

At the end of Section II, I showed that  $\Delta_0 \approx 20$  mas (maximum) for  $\alpha = 0.1$  and other parameters at their nominal values for FAME. A suppression factor of 40 is estimated in Appendix B using a simplified model and  $f=4$ ,  $u=2$ . Thus, before consideration of the effect of TDI,  $\Delta_0 \approx 0.5$  mas for the largest physical effect identified. This is larger than the required single-measurement accuracy for bright stars,  $\sigma_1 = 0.05 \sqrt{N}$  mas, where  $N$  is the number of measurements per mission.  $N$  was estimated by Germain (1995) to be 52 for the FAME concept of that time. Thus,  $\sigma_1 = 0.36$  mas, and only a modest additional suppression is needed from TDI. For now, I consider the subject closed.

In a future memorandum, I may investigate the effect of TDI on biases. Irregularity in CCD clocking, an image path not parallel to the CCD columns, and temporal variations of sensitivity (e.g., ADC noise) could contribute to bias in the estimate in the star coordinate. Also deferred is an investigation of the effect of read noise on the bias.

Appendix A.

$$f \left[ \begin{array}{l} 2 \cdot \text{signum}(\gamma + f - 1) - 2 \cdot f \cdot \text{signum}(-\gamma + f + 1) - f \cdot \text{signum}(-2 + f) + 2 \cdot \text{signum}(-2 + f) - 2 \cdot \text{signum}(2 + f) - 2 \cdot \text{signum}(-\gamma + f - 1) \cdot \gamma - 2 \cdot \text{signum}(\gamma + f - 1) \cdot \gamma - f \cdot \text{signum}(2 \cdot \gamma + f) \dots \\ + \left( 2 \cdot f \cdot \text{signum}(\gamma + f + 1) - f \cdot \text{signum}(2 + f) - 2 \cdot \text{signum}(2 \cdot \gamma + f) \cdot \gamma - 2 \cdot f \cdot \text{signum}(\gamma + f - 1) - 2 \cdot \text{signum}(-\gamma + f + 1) + 4 \cdot f \cdot \text{signum}(f) + 2 \cdot f \cdot \text{signum}(-\gamma + f - 1) - 2 \cdot \text{signum}(-\gamma + f - 1) \dots \right) \\ + 2 \cdot \text{signum}(\gamma + f + 1) + 2 \cdot \text{signum}(-2 \cdot \gamma + f) \cdot \gamma + 2 \cdot \text{signum}(-\gamma + f + 1) \cdot \gamma + 2 \cdot \text{signum}(\gamma + f + 1) \cdot \gamma - f \cdot \text{signum}(-2 \cdot \gamma + f) \end{array} \right]$$

Expression for G(γ,f) picked up from Mathcad as a graphic.

Appendix B.

Here we reconsider the calculation of  $\Delta_0$  with the added requirement that the integral of Eq. (8) be replaced by one with finite limits,  $\pm u\lambda/S$ . An attempt to do an exact calculation with Mathcad caused it to give up. Even with  $\gamma=0$ , the problem proved to be intractable, and involved functions that Mathcad could not evaluate (or even define in “help.” The problem could likely be done by the methods used here, but would be tedious. It is postponed until it is shown to be necessary.) Therefore, here I consider a simplification in which  $G(\gamma,f)$  is replaced by  $G^*(f)$  defined as zero for  $|f| > 2$ , and  $-\text{signum}(f)$  for  $|f| < 2$ . With the help of the following standard expansions

$$\begin{aligned} \sin(kp + \varphi) &= \sin(kp)\cos(\varphi) + \cos(kp)\sin(\varphi) \\ e^{ikp} &= \cos(kp) + i\sin(kp) \end{aligned} \tag{18}$$

the replacement for  $I_v$  of Eq. (8) takes the form

$$\begin{aligned} Z(f,u) &= \sin(\varphi)\text{Re}Q + \cos(\varphi)\text{Im}Q \\ Q &= \int_{-\infty}^{\infty} c b e^{ikp} dp \\ c &= \text{rec}\left(\frac{pS}{u\lambda}\right); \quad b = J_s \frac{\partial J_s}{\partial p} \end{aligned} \tag{19}$$

where the required finite limits of the integral are represented by the *rec* function. Applying the first theorem from page 9, we get

$$Q = \int_{-\infty}^{\infty} C(k-\kappa) B(\kappa) d\kappa \tag{20}$$

where

$$\begin{aligned} C(k) &= \frac{1}{\sqrt{2\pi}} \int_{-\mu\lambda/S}^{\mu\lambda/S} dp e^{ikp} = \\ \frac{1}{\sqrt{2\pi}} \frac{2}{k} \sin\left(\frac{uk\lambda}{S}\right) &= \frac{1}{\sqrt{2\pi}} \frac{2u\lambda}{S} \text{sinc}\left(\frac{uk\lambda}{S}\right) \end{aligned} \tag{21}$$

and

$$B(k) = \frac{1}{\sqrt{2\pi}} \int_{-\infty}^{\infty} dp J_s \frac{\partial J_s}{\partial p} e^{ikp} \quad (22)$$

An integral similar to the above has been evaluated in connection with Eq. (8). To make the connection, we again use Eq. (18), which yields

$$B(k) = \frac{1}{\sqrt{2\pi}} \frac{\pi S^2}{8} i G \left( \gamma, \frac{\lambda k}{\pi S} \right) \quad (23)$$

By combining the above expressions, we obtain

$$Z(f,u) = \cos(\varphi) \frac{u\lambda S}{8} \int_{-\infty}^{\infty} d\kappa \operatorname{sinc} \left( \frac{u\lambda(k-\kappa)}{S} \right) G \left( \gamma, \frac{\lambda\kappa}{\pi S} \right) \quad (24)$$

In the above convolution, we approximate  $G$  by  $G^*$  and change variables ( $k=\pi S f/\lambda$ ,  $\kappa=\pi S \rho/\lambda$ ) to obtain

$$Z^*(f,u) = \cos(\varphi) \frac{\pi S^2}{8} \tilde{G}^* \quad (25)$$

$$\tilde{G}^* = u \int_{-\infty}^{\infty} d\rho \operatorname{sinc}[\pi u(f-\rho)] G^*(\rho)$$

The next step is to evaluate the above integral. We do this in two domains, large  $u$  and large  $f$ . As  $u$  approaches  $\infty$ , one can show that  $\tilde{G}^*$  approaches  $G^*$ , independent of the form of  $G^*$  or of the value of  $f$ . For large  $f$ , one can rearrange Eq. (25) to get

$$\tilde{G}^* = \frac{1}{\pi} [\operatorname{Si}(\pi u(f+2)) + \operatorname{Si}(\pi u(f-2)) - 2\operatorname{Si}(\pi u f)] \quad (26)$$

This can be approximated by using an asymptotic expansion of the Sine Integral (Gautschi and Cahill 1964).

$$\begin{aligned}
\text{Si}(z) &= \int_0^z \frac{\sin(t)}{t} dt = \frac{\pi}{2} - m(z) \cos(z) - n(z) \sin(z) \\
m(z) &\approx \frac{1}{z} \left[ 1 - \frac{2!}{z^2} + \frac{4!}{z^4} - \dots \right] \\
n(z) &\approx \frac{1}{z^2} \left[ 1 - \frac{3!}{z^2} + \frac{5!}{z^5} - \dots \right]
\end{aligned} \tag{27}$$

To lowest order,  $\text{Si}(z) = \pi/2 - \cos(z)/z$ , we get

$$\tilde{G}^* \approx \frac{2}{\pi^2 u} \left[ \frac{\cos(2uf) [f^2(1 - \cos(2\pi u)) - 4] - \sin(2uf) [2f \sin(2\pi u)]}{f(f^2 - 4)} \right] \tag{28}$$

For large  $f$ , the above is dominated by the first term in the big square brackets. If the instrument were looking at a narrow optical band, we could take advantage of the above expression by making  $\cos(2\pi u) \approx 1$ , so as to eliminate the first term. This trick fails in a broad-band instrument (because  $\mu \propto 1/\lambda$  for a fixed physical window size), so in estimating the average value of the above, we take  $\cos(2\pi u) = 0$ .

We are primarily concerned with sensitivity variation with one cycle per pixel. In this case,  $uf$ , which is the number of cycles of perturbation in the observation window, must be an integer. For reasonable values of  $u$  and  $f$ ,  $\cos(2uf)$  does not become small; call it one. Then we find that  $\tilde{G}^* \approx 2/\pi^2 uf$ , which gives a suppression factor of about 40 for  $f=4$  and  $u=2$ . If the coefficient  $\alpha$  in the detector sensitivity factor had a single peak as a function of optical wavelength, the plate scale could be chosen to cause the above to be zero at the offending wavelength. However, this does not seem likely to be the case.

## VII. References.

Gautschi, W. and W.C. Cahill, *Exponential integral and related functions* in Handbook of Mathematical Functions, M. Abramowitz and I.A. Stegun, Eds., National Bureau of Standards, 1964.

Germain, M.E., *Astrometric Accuracy of FAME*, technical memorandum, USNO, 1995.

Jorden, P.R., J-M. Deltorn, and A.P. Oates, *The non-uniformity of CCDs and the effects of spatial undersampling* in Instrumentation in Astronomy VIII, SPIE 2198, D.L. Crawford & E.R. Craine, Eds. 1994.

Jorden, P.R., private communication, 1996.

Marchywka, M. and D.G. Socker, *Modulation transfer function measurement technique for small-pixel detectors*, Applied Optics, 31(34), 1992.

Murison, M.A., private communication, 1997.

Reasenber, R.D., TM96-04, *The Astrometric Information Rate with a Central Obscuration in a Rectangular Aperture*, SAO/PAG technical memorandum, 1996.

## VIII. Acknowledgments

I thank M.A. Murison and J.D. Phillips for reviewing this memorandum in draft form.

## IX. Notes.

1. The reference to a commercial product is for technical communication only, and does not constitute an endorsement of the product.

## X. Distribution.

SAO:

R.W. Babcock  
J.F. Chandler  
J.D. Phillips  
R.D. Reasenber  
I.I. Shapiro

USNO via PKS:

M.E. Germain  
K.J. Johnston  
M.A. Murison  
P.K. Seidelmann  
S.E. Urban

Special:

W.J. Borucki, NASA/ARC  
A. Buffington, UCSD  
J.C. Geary, SAO  
P.R. Jorden, RGO  
D.G. Monet, USNO